

## DEVELOPMENT OF MnO<sub>2</sub>/PANI/SWCNT NANOCOMPOSITE SUPERCAPACITOR ELECTRODE AND INVESTIGATION OF ELECTROCHEMICAL PERFORMANCE

Çağatay ÖZADA <sup>\*,†</sup> 

Merve ÜNAL <sup>\*,†</sup> 

Hakkı ÖZER <sup>Δ,†</sup> 

Murat YAZICI <sup>\*,Δ,†</sup> 

Received: 01.05.2023; revised: 15.09.2023; accepted: 25.09.2023

**Abstract:** In this study, a manganese dioxide (MnO<sub>2</sub>/polyaniline (PANI)/ single-walled carbon nanotube (SWCNT) nanocomposite electrode was prepared for pseudo-supercapacitors. To reduce the internal resistance of the electrode, increase the capacitance stability, and reduce the cost of single-walled carbon nanotubes, SWCNT was subjected to two-step acid etching. The purity of SWCNT was improved from ~95% to 99.98%. In addition, SWCNT was functionalized by this process. Thus, a nanocomposite was formed by coating PANI around SWCNT. MnO<sub>2</sub>/PANI/SWCNT were synthesized using the hydrothermal method. Morphological, chemical and thermal analyses of the synthesized nanocomposite structure were carried out. In addition, X-ray diffraction (XRD) was used to determine the crystal structure. Electrochemical analyses were performed using a three-electrode system in a 1 M KOH electrolyte solution. Cyclic voltammetry (CV) and galvanostatic charge-discharge (GCD) measurements were performed. The capacitance of the nanocomposite electrode at 400 cycles was 314 mF/cm<sup>2</sup>, and the capacitance retention stability was calculated at 73.24%. The results showed that the capacitance stability was high, and the supercapacitor was sensitive to redox reactions.

**Keywords:** Supercapacitor, carbon nanotubes, electrode, polyaniline

### MnO<sub>2</sub>/PANI/SWCNT Nanokompozit Süperkapasitör Elektrot Geliştirilmesi ve Elektrokimyasal Performansının İncelenmesi

**Öz:** Bu makale çalışmasında pseudo-süperkapasitörler için mangan dioksit (MnO<sub>2</sub>) / polianilin (PANI) / tek duvarlı karbon nanotüp (SWCNT) nanokompozit elektrot hazırlanmıştır. Elektrotun iç direncini azaltmak, kapasitans stabilitesini arttırmak ve tek duvarlı karbon nanotüp maliyetini azaltmak için SWCNT iki aşamalı asitle aşındırma çalışması yapılmıştır. SWCNT ~%95 saflıktan %99,98 saflığa ulaştırılmıştır. Ayrıca bu işlemle SWCNT fonksiyonelleştirilmiştir. Böylece SWCNT çevresine PANI kaplanarak nanokompozit oluşturulmuştur. Hidrotermal yöntem ile MnO<sub>2</sub>/PANI/SWCNT sentezlenmiştir. Sentezlenen nanokompozit yapının morfojik, kimyasal ve termal analizleri gerçekleştirilmiştir. Bununla birlikte kristal yapı tayini için X ışını difraksiyometresi (XRD) kullanılmıştır. Elektrokimyasal analizler üçlü elektrot sistemiyle 1 M KOH elektrolit çözeltisinde yapılmıştır. Döngüsel voltametri (CV), galvanostatik şarj-deşarj (GCD) ölçümleri alınmıştır. Nanokompozit elektrodun 400 döngüde kapasitansı 314 mF/cm<sup>2</sup> olarak bulunmuş kapasite tutma kararlılığı ise %73,24 olarak hesaplanmıştır. Yapılan çalışma sonucunda kapasitans kararlılığının yüksek olduğu ve süperkapasitörün redoks tepkimelerine duyarlı olduğu gözlemlenmiştir.

\* Department of Polymer Materials, Institute of Natural Sciences, Bursa Uludağ University, 16059, Nilüfer/BURSA

Δ Department of Automotive Engineering, Engineering Faculty, Bursa Uludağ University, 16059, Nilüfer/BURSA

+ Applied Mechanics and Advanced Material Research Laboratory (AMAMRL) Lab., Bursa Uludağ University, Department of Automotive Engineering, 16059, Nilüfer/BURSA

Corresponding Author: Murat YAZICI, myazici@uludag.edu.tr

**Anahtar Kelimeler:** Süperkapasitör, karbon nanotüp, elektrot, polianilin

## 1. Introduction

Energy storage systems are technologies that allow for energy storage in a form that can be used later (Zhou et al., 2018). These systems store energy from intermittent renewable sources such as solar and wind and provide backup power during blackouts and other power outages (Kaushal et al., 2019). Energy storage systems are critical for integrating renewable energy, providing backup power, optimizing the grid, powering electric vehicles, and reducing energy costs. The demand for energy storage systems is likely to increase as the world transitions to a cleaner, more sustainable energy system. Energy storage systems have a wide range of applications in various sectors. Energy storage systems include batteries, pumped hydro, flywheels, supercapacitors, thermal energy storage, and hydrogen fuel cells (Ibrahim et al., 2008). Batteries are the most common energy storage systems in applications ranging from portable electronics (Dutta et al., 2018) to electric vehicles and grid-scale energy storage.

Supercapacitors, also known as ultracapacitors or electrochemical capacitors, are an increasingly popular energy storage technology that has gained attention for their unique capabilities. Supercapacitors store energy in an electric field, which is created between two electrodes separated by an electrolyte. There are several types of supercapacitors. These include electric double-layer capacitors (EDLC), pseudocapacitors, and hybrid capacitors (Gupta and Kumar, 2019). Different electrode materials have been used in these types of supercapacitors. Carbon-based electrodes have also been used as EDLC supercapacitors. Metal oxides and conductive polymers are often used in pseudocapacitors. Both types of electrodes can be used in hybrid capacitors. The electrolyte is a solution that conducts ions between the electrodes. Supercapacitors have several advantages over traditional batteries (Zhang et al., 2018). They can charge and discharge much faster, typically in seconds or milliseconds, than batteries. They also have a longer cycle life, meaning that they can be charged and discharged many times without degradation. Supercapacitors are more tolerant to extreme temperatures and can operate in a wider range of environments. Supercapacitors have a lower energy density than batteries, meaning they cannot store as much energy per unit of weight or volume (Hashmi et al., 2020). However, they are ideal for applications that require high power output or short-term energy storage, such as regenerative braking in electric vehicles, smoothing out fluctuations in renewable energy sources, and providing backup power for electronic devices.

A pseudocapacitor is a specialized type of supercapacitor that combines the properties of a traditional capacitor and a battery. Unlike conventional supercapacitors, which store energy through the physical separation of charges, pseudocapacitors employ a different mechanism known as faradaic redox reactions. These reactions occur at the interface between the electrode and electrolyte, enabling reversible and rapid electron transfer (Shi et al., 2022). Consequently, pseudocapacitors offer higher energy storage capacities than regular capacitors. There are several critical differences between pseudocapacitors and other supercapacitors. Pseudocapacitors rely on faradaic reactions, while other supercapacitors, such as electrostatic double-layer capacitors, primarily depend on the physical separation of charges at the electrode-electrolyte interface (Mazloomian et al., 2023). Pseudocapacitors provide increased energy storage capabilities owing to the faradaic reactions involved. These reactions involve reversible redox reactions of the ions at the electrode surface, allowing for more excellent charge storage. Pseudocapacitors typically exhibit higher specific capacitance values than other supercapacitors. The specific capacitance refers to the amount of charge that can be stored per unit mass or surface area of the electrode material. Pseudocapacitors have a wider voltage window, meaning they can operate over a broader range of voltages than other supercapacitors. This expanded voltage range enables higher energy storage capacity. Pseudocapacitors commonly employ electrode materials such as transition metal oxides, conducting polymers, or composite materials (Sankar et al., 2022). These materials facilitate faradaic redox reactions and provide high capacitance. Pseudocapacitors exhibit excellent cycling stability with minimal degradation over

multiple charge-discharge cycles. This makes them well-suited for applications that require frequent and reliable energy storage. Pseudocapacitors have garnered significant attention in the field of energy storage owing to their high energy density, rapid charge-discharge rates, and long cycle life. They have applications in various areas, including portable electronics, hybrid vehicles, and renewable energy systems. It is important to note that the specific characteristics and performance of pseudocapacitors can vary depending on factors such as the choice of electrode material, electrolyte composition, and device design. Researchers continue to explore and optimize the properties of pseudocapacitors to enhance their energy storage devices capabilities.

The components of the nanocomposite electrode produced in this study are metal oxide (manganese dioxide), conducting polymer (polyaniline), and carbon (carbon nanotube). Manganese dioxide ( $\text{MnO}_2$ ) is commonly used in pseudocapacitors due to its low cost and environmental friendliness (Liu et al., 2016). In a pseudocapacitor, the energy storage mechanism is based on reversible Faradaic reactions, which involve the transfer of electrons between the electrode material and electrolyte. Additionally,  $\text{MnO}_2$  is abundant and low-cost compared to other redox-active materials, such as ruthenium oxide or conducting polymers. This makes it an attractive material for the large-scale production of supercapacitors.  $\text{MnO}_2$  is environmentally friendly because it is non-toxic and can be easily recycled. These properties make  $\text{MnO}_2$  an attractive electrode material for pseudocapacitors, particularly in applications where high-energy densities are desired. Of the other components, polyaniline (PANI) is a conducting polymer that is commonly used in pseudocapacitors because of its low cost, easy synthesis, and chemical stability. It is an attractive material for large-scale production of supercapacitors. Furthermore, PANI is chemically stable and has good electrical conductivity, making it suitable for use in harsh environments. It is also relatively easy to synthesize and can be produced in various forms, such as nanofibers or films, making it a versatile material for various supercapacitor applications. SWCNTs have a high specific surface area, which enables them to store large amounts of charge at the electrode-electrolyte interface (Gupta and Miura, 2006). They also exhibit excellent electrical conductivity, allowing efficient electron transfer during charge/discharge cycles. Additionally, SWCNTs can be easily functionalized with various functional groups, allowing for the tailoring of their electrochemical properties for specific applications (Li et al., 2004). They are also chemically stable, making them suitable for harsh environments.

Studies in this field have increased over the last ten years. In their study, Yüksel and Ünalın (Yüksel and Unalan, 2015) prepared a  $\text{MnO}_2$ /PANI nanocomposite structure with a single-walled carbon nanotube. SWCNT was coated with manganese, and PANI and poly(3,4-ethylenedioxythiophene) polystyrene sulfonate (PEDOT: PSS) were added as conducting polymers. The electrode was prepared using technical fabric. The results showed a capacitance stability of more than 72% after 1000 cycles. Liu et al. (Liu et al., 2016) discussed the fabrication and electrochemical applications of nanofiber  $\text{MnO}_2$ /PANI/CNT electrodes. This study presents a novel approach for synthesizing ternary coaxial hierarchical nanofibers that exhibit a high specific capacitance and retain their initial capacitance even after 2000 cycles. Although multi-walled carbon nanotubes (MWCNT) were used, the capacitance of this structure was high. In another study, Wu et al. (2019) described the preparation of nanocomposite electrodes and electrochemical testing processes after the purification and functionalization of  $\text{MnO}_2$ /PANI/CNT carbon nanotubes. The nanocomposites were synthesized using a hydrothermal method. After electrochemical testing of the composite, it was observed that it exhibited 90% stability at 1000 cycles. In another study by Huang et al. (Huang et al., 2019), a nanocomposite structure was formed with a polyaniline and manganese dioxide MWCNT structure. In this study, material characterization was performed using morphological and chemical analyses. In addition, electrochemical analysis was performed using cyclic

voltammetry, galvanostatic charge-discharge, and electrochemical impedance spectroscopy. The results showed that the capacitance ratio was 72% after 1000 cycles at a current value of 1 A/g.

In this study, a nanocomposite supercapacitor electrode was fabricated by utilizing the unique advantages of MnO<sub>2</sub>, PANI, and SWCNT structures. For SWCNT, cost reduction and functionalization were performed. Thus, single-walled carbon nanotubes with increased purity give better electrochemical results for supercapacitors. Furthermore, it is aimed at contributing to single-walled carbon nanotube nanocomposite supercapacitors, which are rarely reported in the literature. This study is intended to be a pioneering work in the creation of single-walled manganese-based supercapacitor electrodes. Morphological analysis of the electrode was carried out by TEM. In addition, material characterization was performed using XRD and FTIR. TGA was performed to confirm the purification process accuracy. Electrochemical tests were performed by preparing nanocomposite electrodes on a nickel substrate. Cyclic voltammetry and galvanostatic charge-discharge tests were performed on the electrochemical workstation with a triple electrode system. 1 M potassium hydroxide (KOH) was used as an electrolyte. The results show that the electrode is stable for capacitance.

## 2. MATERIALS AND METHOD

### 2.1. Materials

Single-walled carbon nanotubes ( $\geq 95\%$ ) and ammonium Persulphate (APS) were purchased from Sigma-Aldrich. Aniline monomer was obtained from Boston Chemicals Inc. Nitric acid (HNO<sub>3</sub>), sulfuric acid (H<sub>2</sub>SO<sub>4</sub>), and hydrochloric acid (HCl) were purchased from TEKKİM. Manganese sulfate (MnSO<sub>4</sub>) is also obtained from Merck.

### 2.2. Instrumentation

Thermogravimetric analysis (TGA) measurements were carried out using a TA Instruments/SDT 650 in Bursa Technical University Central research laboratory with a 10°C/min heating rate of 900°C temperature under a dry-air atmosphere. A tunneling transmission electron microscope (TEM) at Middle East Technical University (METU) was used to investigate the nanocomposite morphology. The crystal structure of materials determinations (XRD) was carried out at Rigaku Mini Flex in ENWAIR Energy technologies at a speed of 10°/m at 10-90° 2 $\theta$  angle. In addition, FTIR analysis for the determination of bond formations and functional groups was performed at BUTEKOM.

### 2.3. Electrochemical Analysis

An electrode was prepared from MnO<sub>2</sub>/PANI/SWCNT (active material) nanocomposite for electrochemical tests. Firstly, the active material, acetylene black and PVDF, was mixed in 1-methyl 2-pyrrolidone (NMP) solvent in a ratio of 9:0.5:0.5, and a slurry was prepared. Under vacuum and temperature conditions, this slurry was impregnated on a nickel substrate measuring 10x10 mm, and the test electrode was made. In the electrochemical workstation of the Corrtest brand CS350 model with a three-electrode system, electrochemical tests have been conducted in the lab of Bursa Uludag University Applied Mechanics and Advanced Materials Research Group (UMIMAG). In the electrode system, Ag/AgCl<sup>-</sup> was used as the reference electrode, and platinum wire was used as the counter electrode. 1 M KOH was prepared as the working electrolyte.

## 2.4. Purification and functionalization of SWCNT

The purification process of a single-walled carbon nanotube was carried out with reference to the work of Li et al. (Li et al., 2004). This process takes place in two steps. In the first step, 100 mg of SWCNT was weighted (Figure 1a). Then 50 ml of 3 M HNO<sub>3</sub> was prepared (Figure 1b, Figure 1c). The prepared solution was submerged in an ultrasonic bath for three hours (Figure 1d). The solution was filtered using a vacuum filtering device using a 0.22 m polyester membrane filter (Figure 1e) and washed with ethanol and water. Finally, it was allowed to dry for 8 hours at 120°C in a vacuum oven (Figure 1f).

In the second stage, the sample from the preliminary preparation stage was kept in 50 ml of a 3:1 H<sub>2</sub>SO<sub>4</sub>:HNO<sub>3</sub> solution for 1.5 hours at 60°C on a magnetic stirrer (Figure 1g). It was washed with distilled water and cooled to room temperature at the end of time. It was washed with distilled water until pH was neutral, filtered (Figure 1h), and dried in a vacuum oven at 120°C for 8 hours.

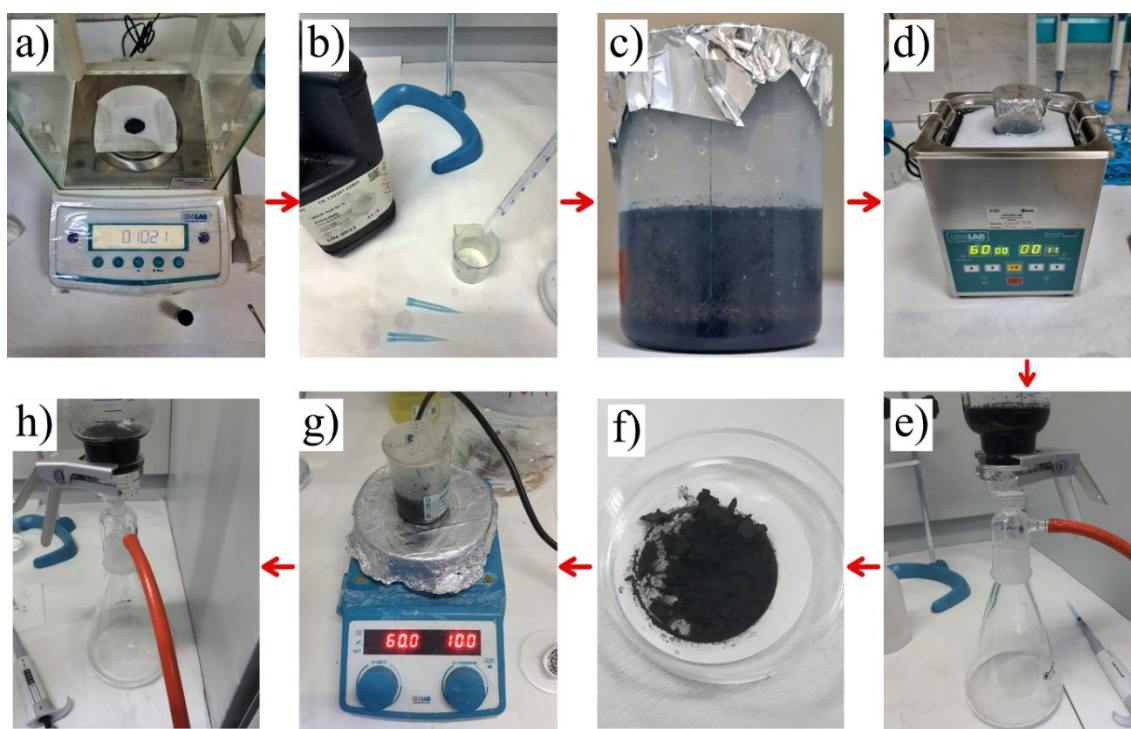


**Figure 1:**

*The SWCNT purification and experimental functionalization steps*

## 2.5. Synthesis of PANI/SWCNT

It is aimed to form a nanocomposite structure with polyaniline using SWCNT with high purity. The experimental steps were as follows: 30 mg of SWCNT obtained from the first study was sonicated in 50 ml of distilled water for 30 minutes. 3 ml of aniline was added, and stirring was performed at room temperature in the solution. 7.2 g of ammonium persulfate (APS) and 1 M HCl were added. The mixture was stirred in a magnetic stirrer for 12 hours at 4°C for polymerization to take place. Finally, the mixture was centrifuged, and the greenish residue was washed with water and ethanol. The mixture was allowed to dry in a vacuum oven at 80°C for 12 hours (Huang et al., 2019).

## 2.6. Synthesis of MnO<sub>2</sub>/PANI/SWCNT Nanocomposite

PANI/SWCNT 270 mg was weighed and sonicated in 216 ml of water for 30 minutes. Then, 1.4 g of MnSO<sub>4</sub> was added to this sonicated solution and stirred at 60°C with a magnetic stirrer. Then, the mixture was reduced to room temperature, and 1.85 g of APS was added. This suspension was stirred at room temperature for 2 hours, then transferred to the hydrothermal reactor and kept in a vacuum oven at 140°C for 12 hours. At the end of the time, the mixture is centrifuged and washed. The final product is obtained by drying in a vacuum oven (Huang et al., 2019).

## 3. RESULTS AND DISCUSSIONS

Morphological analysis of MnO<sub>2</sub>/PANI/SWCNT nanocomposite powder was performed by TEM. Figure 2 clearly shows SWCNT. The polyaniline surrounding the carbon nanotube forms a thickness. Dot appearances deposited on PANI/SWCNT indicate the presence of MnO<sub>2</sub> (Figure 3). It is clear that our research matches the morphological structure of the MnO<sub>2</sub>/PANI/MWCNT electrode fabrication study by Huang et al. (Huang et al., 2019).

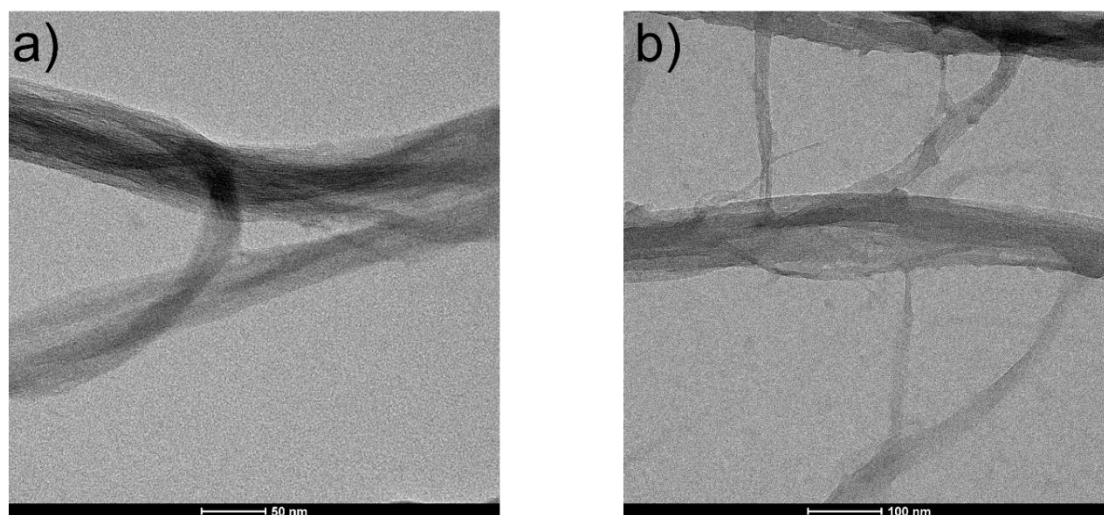


**Figure 2:**

*TEM image of the PANI/SWCNT structure*

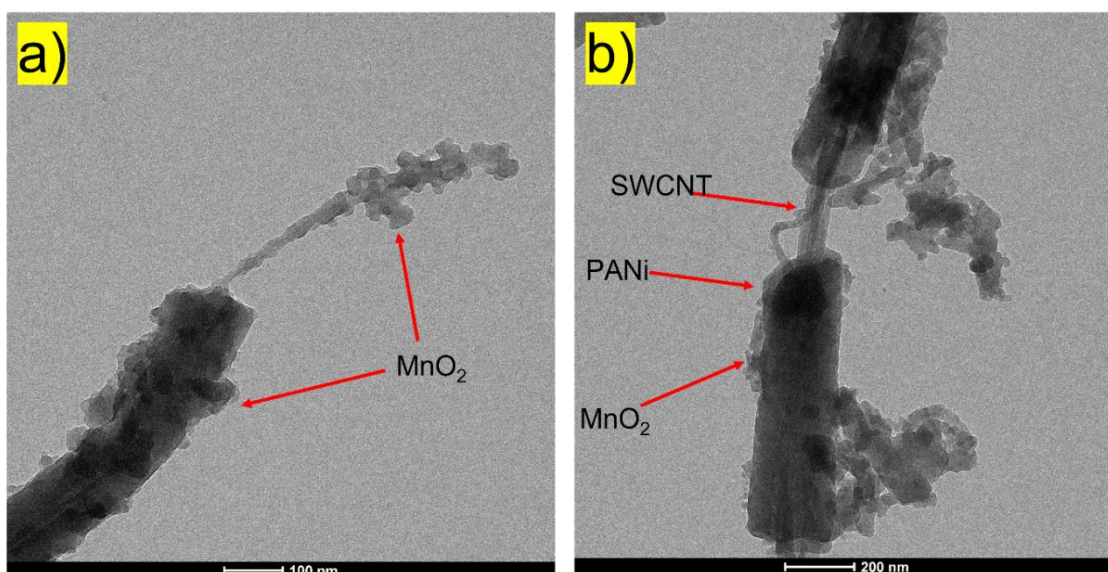


**Figure 3:**

*TEM image of the  $MnO_2/PANI/SWCNT$*

TGA analysis was used to calculate the purification yield for SWCNT obtained after the experiment. TGA conditions were carried out in dry air by heating up to 900°C at a rate of 10°C/min. The TGA analysis before purification is shown in Figure 4. Here, in accordance with the properties of the material, it started to degrade at 476°C. The presence of metal content shows a residual content of 6.45% when the temperature is increased to 900°C.

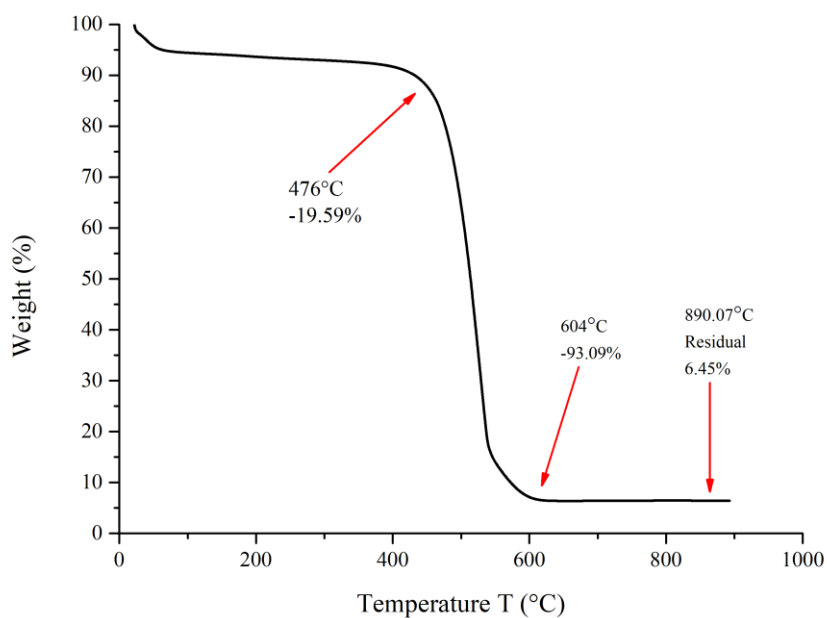


**Figure 4:**

*TGA Analysis of the SWCNT without purification process*

Figure 5 shows the TGA analysis after purification. In the analysis, it was observed that the decomposition temperature increased. In addition, the weight loss is more irregular compared to Figure 4 due to the presence of functional groups. The residue value was found to be 0.02% at the same temperature after this experiment. It is concluded that the purity value of SWCNT reached 99.98%. The purification yield was calculated with the help of Equation 1.

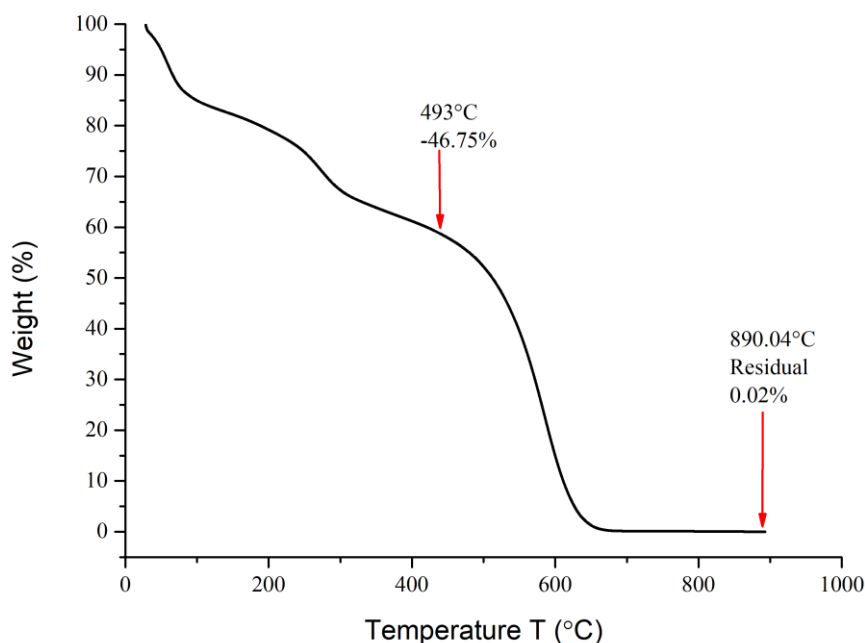


**Figure 5:**

*The SWCNT TGA analysis after purification*

$$\text{Purification yield (\%)} = \frac{w_0 - w_t}{w_0} \cdot 100 \quad (1)$$

Where  $w_0$  is the metal content of unpurified SWCNT (%), and  $w_t$  is the metal content of purified SWCNT (%). According to the result obtained from TGA analysis, the purification efficiency was found to be 99.68%. This result is consistent with the literature (Li et al., 2004).

FTIR analysis was used for the detection of functional groups in combination with SWCNT purification. Figure 6 shows the FTIR spectrum. Considering that functionalization was performed using sulfuric acid and nitric acid in the experimental study, C=C bonding is observed at a wavelength of approximately  $1600 \text{ cm}^{-1}$ . In addition, approximately  $2700 \text{ cm}^{-1}$  peak shows C-H stretching. Finally, the peaks corresponding to  $1100$  and approximately  $800 \text{ cm}^{-1}$  wavelengths indicate C-O bonding. This indicates the presence of oxygen groups on the surface (Yakymchuk et al., 2015).

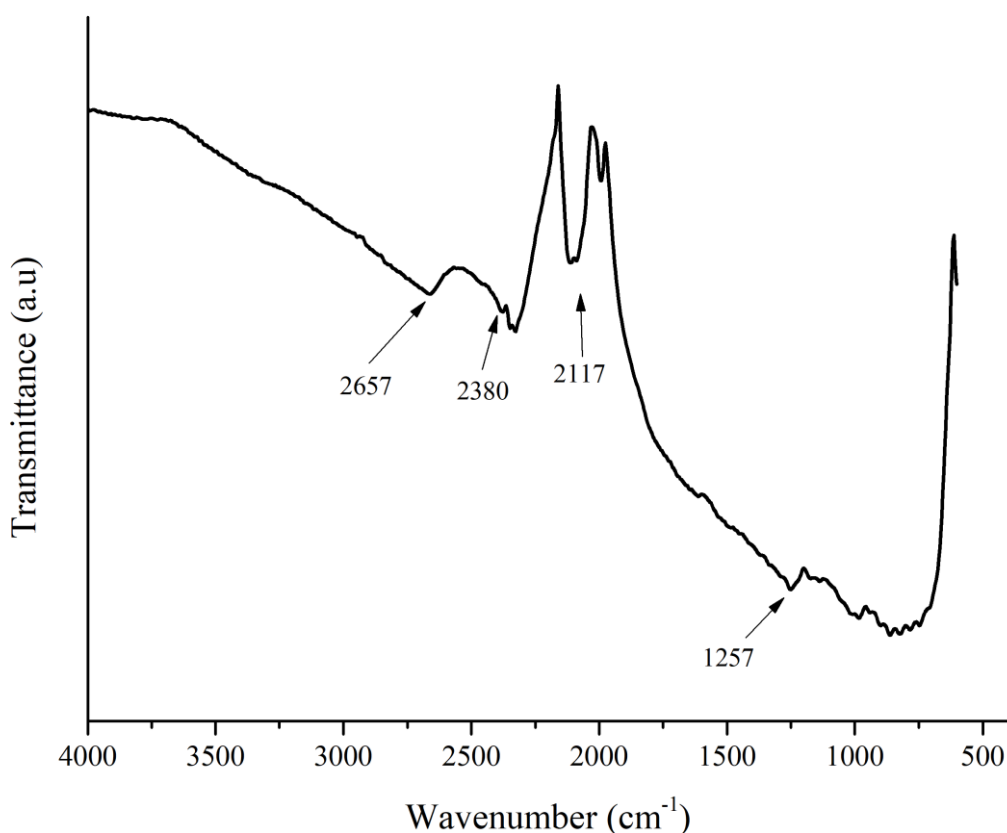


**Figure 6:**

*The SWCNT FTIR Spectrum after Purification*

FTIR analysis of the MnO<sub>2</sub>/PANI/SWCNT structure is shown in Figure 7. The spectrum shows a prominent peak around 3400 cm<sup>-1</sup>. This peak indicates the presence of -NH groups and is produced by polyaniline. In the region of the spectrum between 1700-1750 cm<sup>-1</sup>, a structure like a -C-O-O peak is observed. This peak may indicate the presence of acetic acid derivatives formed by the chemical modification of polyaniline.

Also, distinct peaks are observed in the spectrum between 600-800 cm<sup>-1</sup>. These peaks indicate the presence of SWCNTs and may indicate vibrations of carboxyl groups (-COOH) formed by the chemical exchange of SWCNTs in the nanocomposite structure (Sharma and Sharma, 2013).

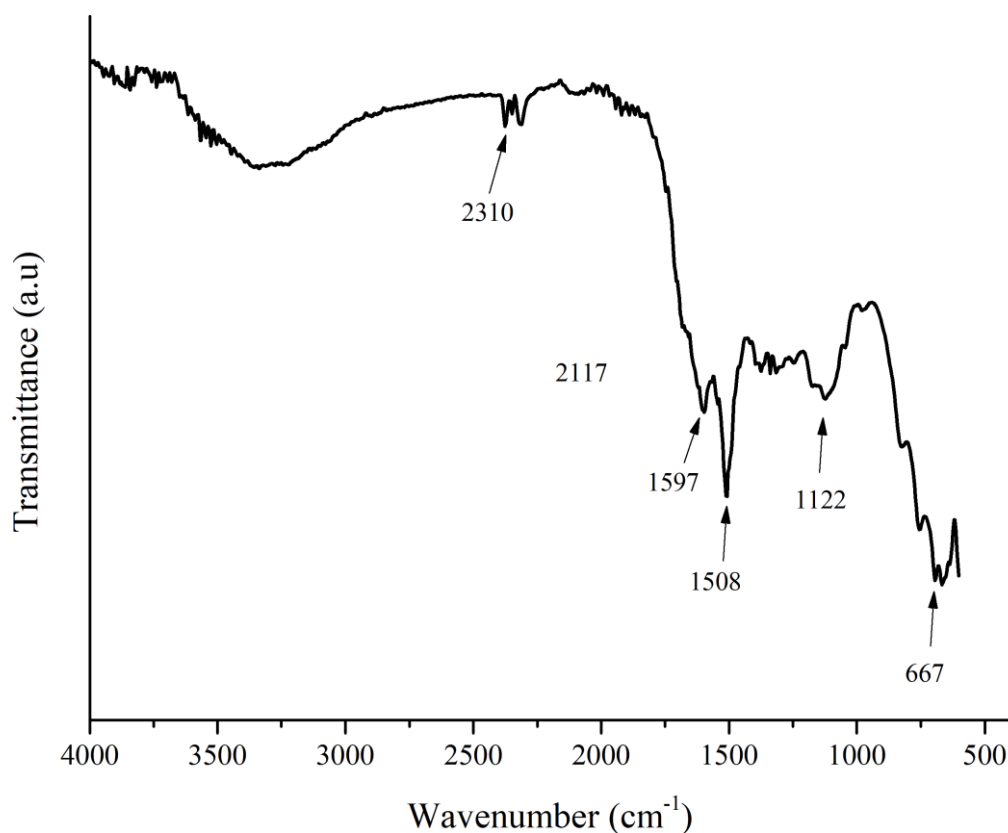


**Figure 7:**

*The MnO<sub>2</sub>/PANI/SWCNT FTIR Spectrum*

XRD method was used to understand the crystal structure determination of the nanocomposite materials. Figure 8 shows the XRD spectrum of PANI with crystal peaks at  $2\theta = 15,3^\circ$ ,  $20,41^\circ$ , and  $25,6^\circ$  corresponding to the (011), (020), and (200) planes indicating the formation of conductive polyaniline (Elnaggar et al., 2017). The  $25,6^\circ$  orthorhombic (110) plane, the characteristic peak for semi-crystalline PANI, is clearly observed. In addition, characteristic refraction peaks are observed at  $2\theta=26,2^\circ$  and  $42,8^\circ$  corresponding to the (002) and (100) crystal planes for SWCNT (Islam et al. 2020). In the MnO<sub>2</sub>/PANI/SWCNT structure, the crystal planes (110), (010), (200), (111), (211), (220), (002), (310), (301) corresponding to angles  $2\theta= 28,6^\circ$ ,  $37,3^\circ$ ,  $41^\circ$ ,  $42,82^\circ$ ,  $56,6^\circ$ ,  $59,3^\circ$ ,  $64,8^\circ$ ,  $67,2^\circ$ ,  $72,2^\circ$  correspond to  $\alpha$ -MnO<sub>2</sub> peaks (JCPDS card PDF file no. 00-024-07359).

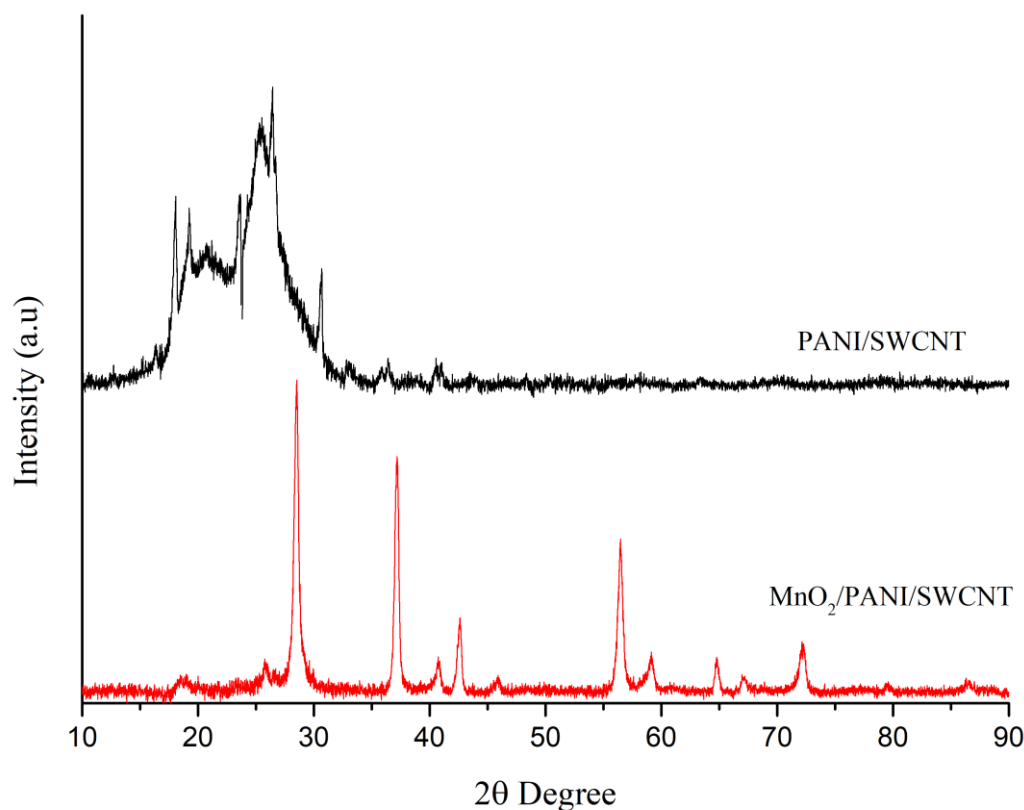


**Figure 8:**

*Compared XRD spectra of the PANI/SWCNT and the MnO<sub>2</sub>/PANI/SWCNT structures*

### 3.1. Electrochemical Tests

Scan rates of 5 mV/s, 10 mV/s, 50 mV/s, and 100 mV/s were used during the electrochemical test. The potential range was taken as (-0.6V-0.6 V). The active material loading weight of the electrode was calculated at 3 mg. The test results show that the current values on the electrode increase with increasing scan rate. This shows the effect of the scan rate on the electrochemical behavior of the electrode (Figure 9). The graph clearly shows the anodic and cathodic peaks. The peaks on the graph represent the points where electrochemical reactions occur. Anodic peaks occur on the positive side of the curve, while cathodic peaks are observed on the negative side of the curve. This indicates the presence of redox reactions. In the study by Wu et al. (Wu et al. 2019), a CV test was applied for the MnO<sub>2</sub>/PANI/MWCNT electrode at 5-80 mV/s. The curves show similar characteristics to this study. The weak rectangularity of the composites is probably attributed to the close bonding of MnO<sub>2</sub> and conductors (CNTs and PANI), which can minimize the contact resistance between them, thus facilitating the Faraday processes of electrochemically active species (Li et al., 2004). Chen et al. (Chen et al., 2013) performed CV testing of activated carbon/manganese dioxide/polyaniline electrode in a potential window of -0.2V-0.8 mV and a scan rate of 20 mV/s. In the graph obtained because of the test, they observed redox transitions between the polaronic form and the leucomeraldin form of polyaniline at 0.18 V - 0.6 peaks. In the CV test in our study, peaks are observed at close

points. However, the shifts in the peak values are due to the potential window we used in our study.

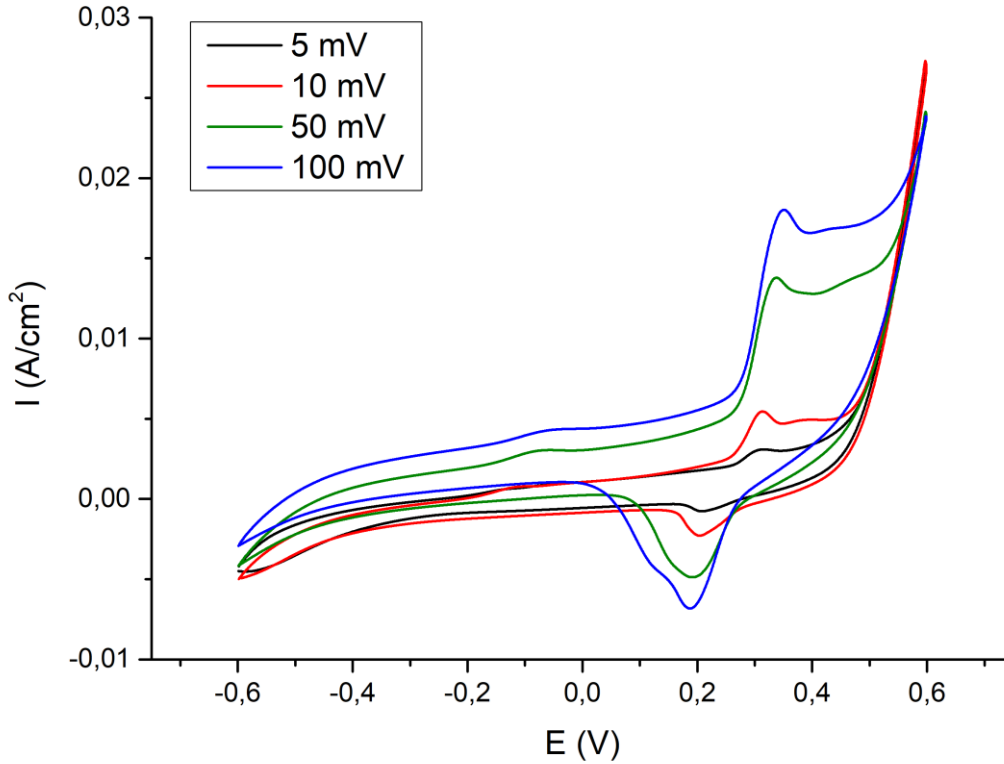


**Figure 9:**

*Cyclic voltammetry testing of nanocomposite electrode*

An electrode surface area of  $1 \text{ cm}^2$  was used in the galvanostatic charge-discharge test. The loading weight of the active material ( $\text{MnO}_2/\text{PANI}/\text{SWCNT}$ ) was calculated at 3 mg. The test conditions were in the potential window range of 0.4-0.25 V, and the scan rate was taken as 1 mA. In addition, the test was continued for 500 cycles. The graph given in Figure 10 shows the results of the galvanostatic charge-discharge test. This test is a method used to measure the capacitance and energy storage performance of the electrode. The symmetric galvanostatic curves show reversible redox reactions. Charge and discharge times as a function of time are also shown. The fluctuation in the curves is an indication of internal resistance in the supercapacitor. When compared with the literature, it is understood that these internal resistances cause lower capacitance. However, the same continuation of the curves is an indication that the supercapacitor is stable. The fact that the galvanostatic charge-discharge curves are not triangular is evidence that the electrode material shows non-electrostatic behavior (Iqbal et al., 2020).

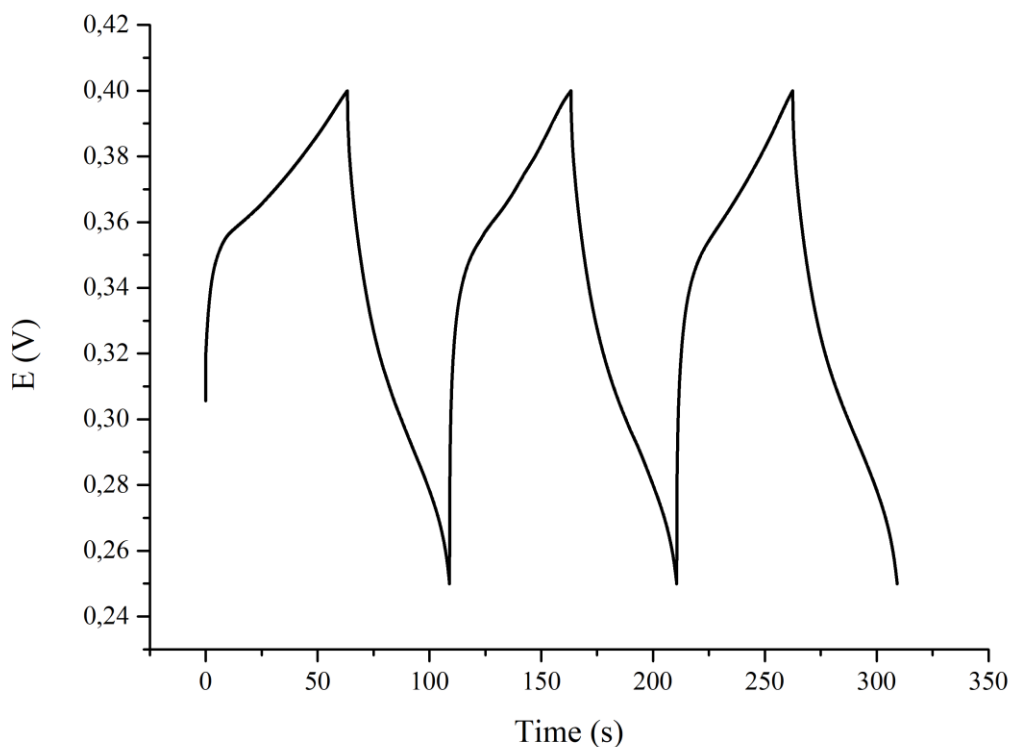


**Figure 10:**

*Galvanostatic charge-discharge curve*

The graph showing the specific charge and discharge capacitance of the supercapacitor is shown in Figure 11. The area of the electrode was taken as 1 cm<sup>2</sup>. The test was performed with a current density of 1mA/cm<sup>2</sup> and a voltage window of 0.4-0.25. The active material loading weight of the electrode is 3 mg. The following Equation 2 was used for calculations (Himi et al., 2023):

$$C = \frac{I\Delta t}{A\Delta v} \quad (2)$$

In this formula, I is the applied current value,  $\Delta t$  is the discharge time, m is the loading amount, and  $\Delta V$  is the voltage window. According to this formula, the specific discharge capacitance was calculated at 314 mF/cm<sup>2</sup>. Compared to PANI/MnO<sub>2</sub> (Tian et al., 2023) and MnO<sub>2</sub>/CNT/paper (Dong et al., 2016) electrodes in the literature, the addition of PANI and SWCNT nanocomposite increases the areal capacitance. The capacitance retention value of the supercapacitor after 400 cycles was calculated at 73.24%.

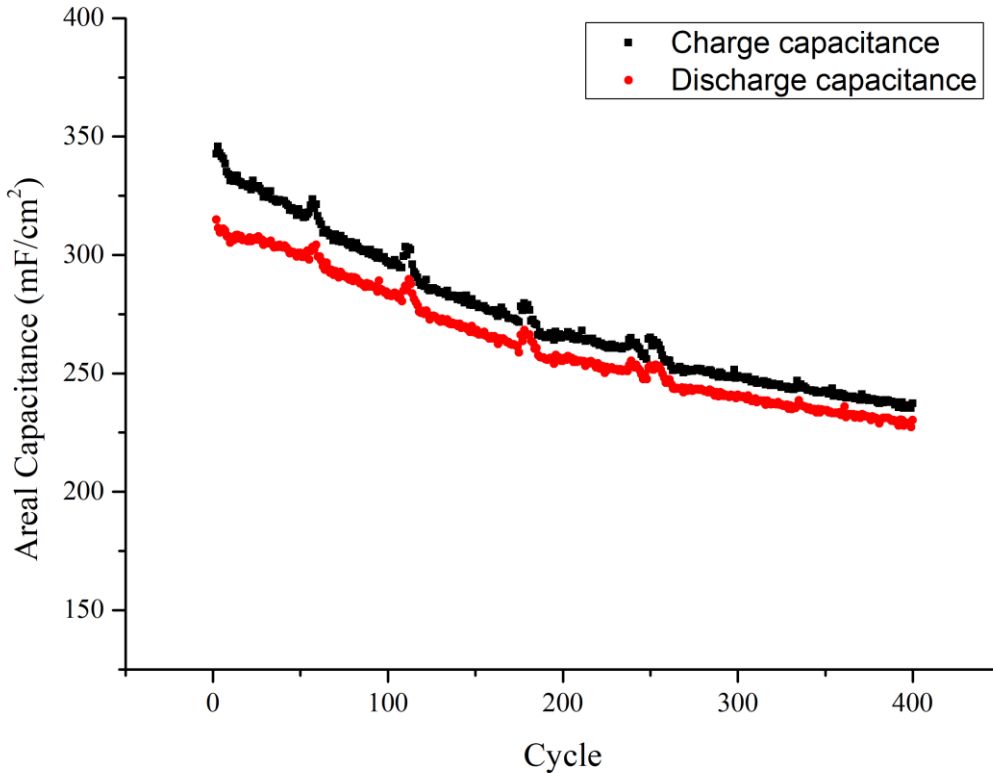


**Figure 11:**

*The MnO<sub>2</sub>/PANI/SWCNT specific capacitance*

#### 4. CONCLUSION

In this work starts with the purification step of the single-walled carbon nanotube. The purification step of the SWCNT structure was demonstrated by TGA analysis. 99.68% purification efficiency is a significant value for supercapacitors. The increase in the purity rate leads to an improvement in the charge-discharge stability of the supercapacitor. Material characterizations after synthesis of MnO<sub>2</sub>/PANI/SWCNT nanocomposite clearly show the nanocomposite formation. Electrochemical tests performed with the electrode obtained from this nanocomposite powder showed the capacitance stability of the supercapacitor. Cyclic voltammetry tests prove that the supercapacitor responds very well to redox reactions. The galvanostatic charge-discharge test shows the charge and discharge times of the supercapacitor. The duration of the charge stored by the supercapacitor and the discharge time of this charge was measured by this test. After 400 cycles of charge-discharge of this supercapacitor, capacitance measurements were performed. It was observed that the supercapacitor, whose area capacitance value was calculated as approximately 314 mF/cm<sup>2</sup>. The capacitance retention value was calculated at 73.24%. This shows that the capacitance of the supercapacitor is stable for long cycles. The results show that the MnO<sub>2</sub>/PANI/SWCNT electrode supercapacitor has improvable properties. Especially in long cycles, it can be aimed to increase the capacitance by

maintaining the stable capacitance state. This paper presents the advanced properties of the nanocomposite electrode made with SWCNT and provides support for further studies.

### CONFLICT OF INTEREST

Authors approve that, to the best of their knowledge, there is not any conflict of interest or common interest with an institution/organization or a person that may affect the review process of the paper.

### AUTHOR CONTRIBUTION

Çağatay ÖZADA is determining the concept and design process of the research, experimental and research management, data collection, and analysis. Merve ÜNAL is determining the experimental process of the research. Hakkı ÖZER is determining the materials characterization and data collection. Murat YAZICI is determining data collection, analysis, and management.

### ACKNOWLEDGMENT

This project work was supported by TUBITAK 1002-B with project code 122M934 and Bursa Uludag University Scientific Research Projects Unit with project code FOA-2021-681. In addition, Çağatay ÖZADA, one of the authors, is supported by TÜBİTAK 2211/C and YÖK 100/2000 doctoral scholarship program. Merve ÜNAL is supported by YÖK 100/2000 doctoral scholarship program.

### REFERENCES

1. Chen, Wei (2013) MnO<sub>2</sub> Based Nanostructures for Supercapacitor Energy Storage Applications. Doctor of Philosophy.
2. Dong, Liubing; Xu, Chengjun; Li, Yang; Pan, Zhengze; Liang, Gemeng; Zhou, Enlou et al. (2016) Breathable and Wearable Energy Storage Based on Highly Flexible Paper Electrodes. In *Advanced materials (Deerfield Beach, Fla.)* 28 (42), pp. 9313–9319. doi: 10.1002/adma.201602541.
3. Dutta, Shibsankar; Pal, Shreyasi; De, Sukanta (2018) Few-layered MnO<sub>2</sub>/SWCNT hybrid in-plane supercapacitor with high energy density. In. 2ND INTERNATIONAL CONFERENCE ON CONDENSED MATTER AND APPLIED PHYSICS (ICC 2017). Bikaner, India, 24–25 November 2017: Author(s) (AIP Conference Proceedings), p. 30145.
4. Elnaggar, Elsayed M.; Kabel, Khalid I.; Farag, Ahmed A.; Al-Gamal, Abdalrhman G. (2017) Comparative study on doping of polyaniline with graphene and multi-walled carbon nanotubes. In *J Nanostruct Chem* 7 (1), pp. 75–83. doi: 10.1007/s40097-017-0217-6.
5. Gupta, Vinay; Kumar, S. (2019) MnO<sub>2</sub>/SWCNT buckypaper for high performance supercapacitors. In *Journal of Energy Storage* 26, p. 100960. doi: 10.1016/j.est.2019.100960.
6. Gupta, Vinay; Miura, Norio (2006) Polyaniline/single-wall carbon nanotube (PANI/SWCNT) composites for high performance supercapacitors. In *Electrochimica Acta* 52 (4), pp. 1721–1726. doi: 10.1016/j.electacta.2006.01.074.
7. Hashmi, Safir Ahmad; Yadav, Nitish; Singh, Manoj Kumar (2020) Polymer Electrolytes for Supercapacitor and Challenges. In Tan Winie, Abdul K. Arof, Sabu Thomas (Eds.): *Polymer Electrolytes*: Wiley, pp. 231–297.

8. Himi, M. Ait; Sghiouri, A.; Youbi, B.; Lghazi, Y.; Amarray, A.; Aqil, M. et al. (2023) Effect of applied potential on supercapacitor performances of manganese oxide nanomaterials electrodeposited on indium tin oxide substrate. In *Journal of Energy Storage* 61, p. 106711. doi: 10.1016/j.est.2023.106711.
9. Huang, Yingying; Lu, Jinlin; Kang, Shumei; Weng, Duo; Han, Lu; Wang, Yongfei (2019) Synthesis and Application of MnO<sub>2</sub>/PANI/MWCNT Ternary Nanocomposite as an Electrode Material for Supercapacitors. In *International Journal of Electrochemical Science* 14 (9), pp. 9298–9310. doi: 10.20964/2019.09.86.
10. IBRAHIM, H.; Ilınca, A.; PERRON, J. (2008) Energy storage systems—Characteristics and comparisons. In *Renewable and Sustainable Energy Reviews* 12 (5), pp. 1221–1250. doi: 10.1016/j.rser.2007.01.023.
11. Iqbal, Javed; Ansari, Mohammad Omaish; Numan, Arshid; Wageh, S.; Al-Ghamdi, Ahmed; Alam, Mohd Gulfam et al. (2020) Hydrothermally Assisted Synthesis of Porous Polyaniline@Carbon Nanotubes-Manganese Dioxide Ternary Composite for Potential Application in Supercapattery. In *Polymers* 12 (12). doi: 10.3390/polym12122918.
12. Islam, Rakibul; Papathanassiou, Anthony N.; Chan-Yu-King, Roch; Gors, Carole; Roussel, Frédérick (2020) Competing charge trapping and percolation in core-shell single wall carbon nanotubes/ polyaniline nanostructured composites. In *Synthetic Metals* 259, p. 116259. doi: 10.1016/j.synthmet.2019.116259.
13. Kaushal, Indu; Sharma, Ashok K.; Saharan, Priya; Sadasivuni, Kishor Kumar; Duhan, Surender (2019) Superior architecture and electrochemical performance of MnO<sub>2</sub> doped PANI/CNT graphene fastened composite. In *J Porous Mater* 26 (5), pp. 1287–1296. doi: 10.1007/s10934-019-00728-8.
14. Li, Yu; Zhang, Xiaobin; Luo, Junhang; Huang, Wanzhen; Cheng, Jipeng; Luo, Zhiqiang et al. (2004) Purification of CVD synthesized single-wall carbon nanotubes by different acid oxidation treatments. In *Nanotechnology* 15 (11), pp. 1645–1649. doi: 10.1088/0957-4484/15/11/047.
15. Liu, Wenjie; Wang, Shishuang; Wu, Qianhui; Huan, Long; Zhang, Xiue; Yao, Chao; Chen, Ming (2016) Fabrication of ternary hierarchical nanofibers MnO<sub>2</sub>/PANI/CNT and their application in electrochemical supercapacitors. In *Chemical Engineering Science* 156, pp. 178–185. doi: 10.1016/j.ces.2016.09.025.
16. Mazloomian, Katrina; Lancaster, Hector J.; Howard, Christopher A.; Shearing, Paul R.; Miller, Thomas S. (2023) Supercapacitor Degradation: Understanding Mechanisms of Cycling-Induced Deterioration and Failure of a Pseudocapacitor. In *Batteries & Supercaps* 6 (8), Article e202300214. doi: 10.1002/batt.202300214.
17. Sankar, A.; Chitra, S. Valli; Jayashree, M.; Parthibavarman, M.; Amirthavarshini, T. (2022) NiO nanoparticles/graphene nanocomposite as high-performance pseudocapacitor electrodes: Design and implementation. In *Diamond and Related Materials* 122, p. 108804. doi: 10.1016/j.diamond.2021.108804.
18. Sharma, Ashok K.; Sharma, Yashpal (2013) p-toluene sulfonic acid doped polyaniline carbon nanotube composites: synthesis via different routes and modified properties. In *J. Electrochem. Sci. Eng.* doi: 10.5599/jese.2013.0029.
19. Shi, Chenglong; Sun, Junlong; Pang, Youyong; Liu, YongPing; Huang, Bin; Liu, Bo-Tian (2022) A new potassium dual-ion hybrid supercapacitor based on battery-type Ni(OH)<sub>2</sub> nanotube arrays and pseudocapacitor-type V<sub>2</sub>O<sub>5</sub>-anchored carbon nanotubes electrodes. In

*Journal of colloid and interface science* 607 (Pt 1), pp. 462–469. doi: 10.1016/j.jcis.2021.09.011.

20. Tian, Menghan; Liu, Xueqing; Diao, Xungang; Zhong, Xiaolan (2023) High performance PANI/MnO<sub>2</sub> coral-like nanocomposite anode for flexible and robust electrochromic energy storage device. In *Solar Energy Materials and Solar Cells* 253, p. 112239. doi: 10.1016/j.solmat.2023.112239.
21. Wu, Huatao; La, Ming; Li, JinHui; Han, Yongjun; Feng, Yunxiao; Peng, Qinlong; Hao, Chengjun (2019) Preparation and electrochemical properties of MnO<sub>2</sub>/PANI-CNTs composites materials. In *Composite Interfaces* 26 (8), pp. 659–677. doi: 10.1080/09276440.2018.1526592.
22. Yakymchuk, Olena M.; Perepelytsina, Olena M.; Dobrydnev, Alexey V.; Sydorenko, Mychailo V. (2015) Effect of single-walled carbon nanotubes on tumor cells viability and formation of multicellular tumor spheroids. In *Nanoscale research letters* 10, p. 150. doi: 10.1186/s11671-015-0858-7.
23. Yuksel, Recep; Unalan, Husnu Emrah (2015) Textile supercapacitors-based on MnO<sub>2</sub>/SWNT/conducting polymer ternary composites. In *Int. J. Energy Res.* 39 (15), pp. 2042–2052. doi: 10.1002/er.3439.
24. Zhang, Qun-Zheng; Zhang, Dian; Miao, Zong-Cheng; Zhang, Xun-Li; Chou, Shu-Lei (2018) Research Progress in MnO<sub>2</sub>-Carbon Based Supercapacitor Electrode Materials. In *Small (Weinheim an der Bergstrasse, Germany)* 14 (24), e1702883. doi: 10.1002/sml.201702883.
25. Zhou, Lei; Li, Chunyang; Liu, Xiang; Zhu, Yusong; Wu, Yuping; van Ree, Teunis (2018) Metal oxides in supercapacitors. In : *Metal Oxides in Energy Technologies*: Elsevier, pp. 169–203.

